High SNR DCE Imaging for Whole-Brain Perfusion Assessment

Philippe Gauderon[1,2], Marina Salluzzi[2,3], Michel Louis Lauzon[2,3], Michael Richard Smith[1,4], and Richard Frayne[2,3]

[1]*Biomedical Engineering, University of Calgary, Calgary, Alberta, Canada,* [2]*Seaman Family MR Research Centre, Calgary, Alberta, Canada,* [3]*Radiology, University of Calgary, Calgary, Alberta, Canada,* [4]*Electrical and Computer Engineering, University of Calgary, Calgary, Alberta, Canada*

INTRODUCTION: Dynamic susceptibility contrast (DSC) MR imaging is a standard technique for the assessment of cerebral perfusion. Quantitative hemodynamic parameters, *e.g.,* cerebral blood flow (CBF), are commonly derived from DSC data using tracer kinetics models. Nevertheless, an increasing number of studies have highlighted various shortcomings that hinder reliable quantification of cerebral perfusion (1-3). Dynamic contrast-enhanced (DCE) MR has been suggested as an alternative to DSC, as it is able to overcome many of these shortcomings. Initial studies using sampling strategies for the acquisition of 4 to 6 slices only (4,5), demonstrated that DCE is able to provide quantitative CBF estimates. Here we propose and assess a whole-brain DCE perfusion protocol with high SNR – a necessary requirement given that the contrast agent-induced DCE signal enhancement is known to be small in cerebral tissue.

METHODS: The DCE acquisition was performed in a healthy volunteer using a 3 T scanner (Discovery MR750; GE Healthcare, Waukesha, WI) with a 32-channel head-coil. Three-dimensional (3D) SPGR sequences were used for the precontrast B_1 and T_1 measurements, as well as for the DCE acquisition. All acquisitions used a FOV of 240 mm × 192 mm and a slice thickness of 5 mm. The images from all acquisitions were reconstructed to 256 × 256 in plane and were zero-fill interpolated by a factor of 2 in the *z*-direction. Precontrast T_1 values were measured using the variable flip angle method (6,7) with a TR/TE = 7.5 ms/1.2 ms, FA_1 = 4° and FA_2 = 18°. Its acquisition matrix was 80 × 64 × 30, resulting in a voxel size of 3 mm × 3 mm × 5 mm. The dual TR method (7) with TE/FA = 3.1 ms/60°, TR_1 = 10 ms and TR_2 = 50 ms was used to generate B_1 maps. For this acquisition, the acquisition matrix was reduced to 40 × 32 × 30, resulting in a voxel size of 6 mm × 6 mm × 5 mm. The acquisition time for the B_1 and T_1 mapping was 58 s and 30 s, respectively. The DCE implementation combined a SPGR sequence with variable rate *k*-space sampling, *i.e.,* TRICKS (8), and parallel imaging, *i.e.,* SENSE. It was observed that for the same acquisition time per frame, parallel imaging with increasing acceleration factors provided increasingly more SNR, provided that the preserved acquisition time from collecting less phase encodes is spent on longer TR and simultaneously lower receiver bandwidths (RBW). The TR/TE/FA were 9 ms/3.9 ms/39° and the acquisition matrix was 86 × 70 × 30, resulting in a voxel size of 2.8 mm × 2.8 mm × 5 mm. Consequently the RBW was ± 6.41 kHz. The use of a SENSE factor of 3 together with TRICKS resulted in the reconstruction of 48 temporal frames, one frame every 1.8 s. The contrast agent (0.075 mM/kg of Gadovist, Bayer) was injected at 5 mL/s. The B_1 maps were used to improve the accuracy of the T_1 maps, as described in (7). From the T_1 precontrast measurements and the contrast agent-induced signal enhancement curves, quantitative contrast agent concentration curves were generated for each voxel (9). An arterial input function was then selected. Using a deconvolution algorithm based on Tikhonov regularization and the indicator-dilution theory, quantitative perfusion estimates were calculated.

RESULTS: Fig. 1 shows voxel-wise SNR and ΔSNR (*i.e.,* CNR) maps calculated from the standard deviation of 12 DCE baseline frames (before contrast arrival). The SNR in white matter (WM) was found to be 136 ± 53 and in gray matter (GM) 150 ± 60. The ΔSNR, defined as the maximal signal difference divided by the baseline standard deviation, was measured to be 14 ± 7 in WM and 37± 19 in GM. Perfusion maps were successfully generated for the whole brain of the subject (Fig 2). Fig. 3 shows representative CBF, cerebral blood volume (CBV) and mean-transit time (MTT) maps together with reference data of a selected slice. It can be observed that the regions with increased fractional anisotropy (*i.e.,* the WM) correspond well with the low CBF and CBV areas. The CBF in WM was found to be 15.1 ± 4.9 mL/100 g/min, the CBV 2.2 ± 0.6 mL/100 g and the MTT 9 ± 1.9 s. In GM the CBF was measured to be 37.9 ± 11.1 mL/100 g/min, the CBV 4.9 ± 1.5 mL/100 g and the MTT 7.8 ± 0.9 s. While the generated CBV values correspond well with literature values (10), the CBF values were slightly underestimated and the MTT values therefore overestimated.

CONCLUSION: A whole-brain perfusion protocol for the acquisition of DCE data with high SNR was successfully implemented and tested. The high SNR allowed the generation of robust quantitative perfusion estimates. The slight CBF underestimation is expected to be a consequence of the deconvolution process. To our knowledge, this implementation is the first to demonstrate that quantitative whole-brain DCE perfusion imaging is feasible.

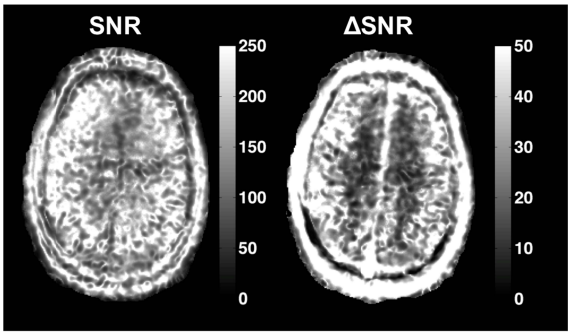

Fig 1: Voxel-wise SNR and ΔSNR maps of the same slice as shown in Fig. 2.

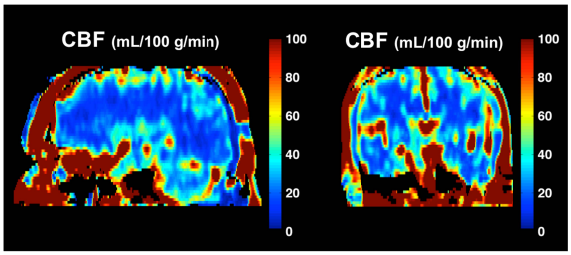

Fig 2: Sagittal and coronal CBF maps illustrating the whole-brain coverage of the proposed acquisition protocol.

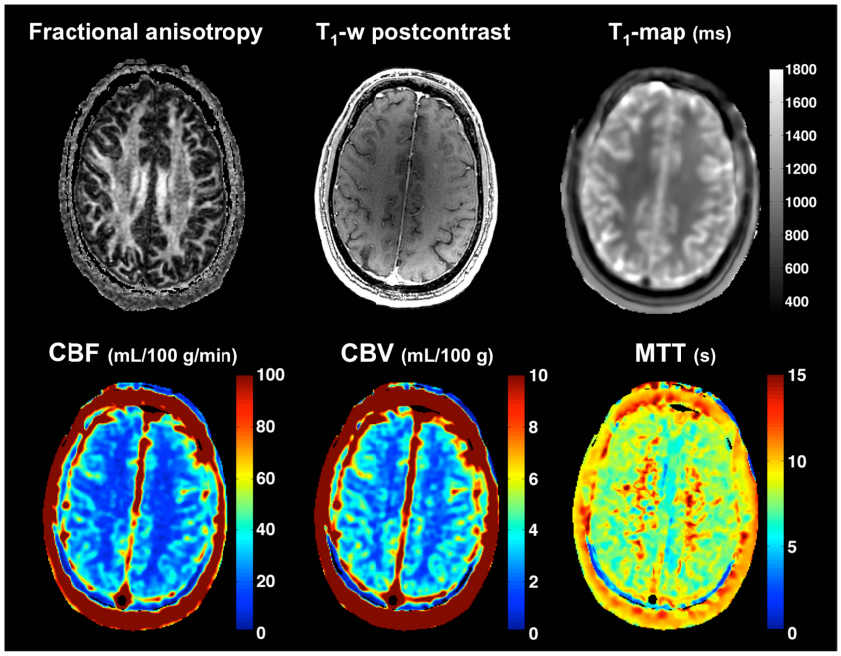

Fig 3: Quantitative CBF, CBV and MTT maps for one selected slice (bottom row). Fractional anisotropy of diffusion and T_1-weighted postcontrast images are shown together with the processed T_1-map of the same slice (top row).

REFERENCES: **(1)** Kiselev, *J Magn Reson Imaging* 2005;22: 693. **(2)** van Osch, *et al.*, *J Magn Reson Imaging* 2005;22: 704. **(3)** Calamante, *Top Magn Reson Imaging* 2010;21: 75. **(4)** Larsson, *et al.*, *J Magn Reson Imaging* 2008;27: 754. **(5)** Sourbron, *et al.*, *Magn Reson Med* 2009;62: 205. **(6)** Deoni, *et al.*, *Magn Reson Med* 2005;53: 237. **(7)** Treier, *et al.*, *Magn Reson Med* 2007;57: 568. **(8)** Frayne, *et al.*, *Top Magn Reson Imaging* 1996;8: 366. **(9)** Schabel, *et al.*, *Phys Med Biol* 2008;53: 2345. **(10)** Rostrup, *et al.*, *Neuroimage* 2005;24: 1.